

Multiple ionization of iron by electron impact

M B Shah, P McCallion, K Okuno† and H B Gilbody

Department of Pure and Applied Physics, The Queen's University of Belfast, Belfast, UK

Received 16 November 1992, in final form 15 February 1993

Abstract. We have used a pulsed crossed beam technique incorporating time-of-flight spectroscopy of the collision products to study the electron impact ionization of ground state Fe atoms. Relative cross sections σ_n for the formation of 1 to 4 times ionized iron have been measured within the energy range 8–1250 eV. Individual cross sections have been obtained by normalization to lower energy values of σ_2 previously measured by Freund *et al* using a fast crossed beam experiment where analysis was complicated by the presence of metastable atoms in Fe beams. Measured cross sections exhibit evidence of contributions from inner shell electrons. Our high energy values of σ_1 are in excellent agreement with theoretical predictions based on the first Born approximation.

1. Introduction

In previous work in this laboratory (Shah *et al* 1987) we used a pulsed crossed beam technique incorporating time-of-flight spectroscopy for measurements of the electron impact ionization cross section of atomic hydrogen with high precision over a wide energy range. The method is ideally suited to measurements with unstable species such as atomic hydrogen in the form of thermal energy beams. However we have also shown in measurements on He and Ar (Shah *et al* 1988, McCallion *et al* 1992a) that it can also be applied with advantage to study multiple ionization of stable target species where the results of other methods often exhibit significant discrepancies. We have also demonstrated in measurements with Mg (McCallion *et al* 1992b) that, by the use of a specially developed high temperature oven source, studies of the multiple ionization of metallic species are also feasible.

In the present work we have studied the processes



for $n=1$ to 4 at impact energies in the range 8–1250 eV. Accurate ionization cross sections for iron are important in astrophysics. In addition, reliable data are required for a better understanding of impurity transport in high temperature fusion plasmas (Janev 1990). The only previous measurements on iron have been carried out by Freund *et al* (1990) using the fast crossed beam technique. Measured cross sections were limited to $n=1$ and 2 only and energies up to 200 eV. In these measurements, the electron beam was crossed with a 3 keV beam of Fe atoms prepared by charge transfer neutralization of Fe^+ ions in a gas target. Measurement of the fractional yield of Fe^{n+} ions from a region where the collision volume and density profiles are well defined then allowed absolute cross sections to be determined. However, Freund *et al* (1990)

† Permanent address: Tokyo Metropolitan University, Tokyo, Japan.

obtained evidence of significant ionization below the ground state threshold indicating that their Fe beams contained a substantial admixture of metastable species. They concluded that their measured Fe^+ formation cross sections were therefore of 'questionable significance' since they contained unknown contributions from many metastable states of Fe.

The present pulsed crossed beam method utilized ground state thermal energy beams of Fe and therefore avoided the problem of metastable contamination inherent in the fast crossed beam method used by Freund *et al* (1990). However, in our method the determination of accurate absolute cross sections is a much more difficult problem primarily because of the difficulty in accurately determining the absolute flux of the thermal energy Fe beam. For this reason, our measurements have been limited to an accurate determination of the relative cross sections for Fe^{n+} production for $n = 1$ to 4. The determination of individual cross sections from these measurements requires normalization to other data.

2. Experimental approach

2.1. General description

The crossed beam apparatus was basically the same as that described previously (Shah *et al* 1987, McCallion *et al* 1982b) and only the essential features need to be summarized here.

A scheme of the crossed beam arrangement and electronics for signal recovery is given in figure 1 of Shah *et al* (1987). The electron gun was triggered by a pulse generator to provide electron pulses of 200 ns duration at a repetition rate of about 10^5 pulses/s. The pulsed beam of electrons was arranged to intersect (at 90°) a beam of Fe atoms effusing from an oven source. The crossed beam region was located in a differentially pumped vacuum chamber maintained at a pressure of about 5×10^{-8} Torr.

Immediately after the transit of each pulse of electrons through the Fe atom beam slow Fe^{n+} products of ionization were swept out of the crossed beam region by a pulsed electric field. A field of 15 V cm^{-1} applied between two high transparency grids placed on either side of the crossed beam region was found to be sufficient to ensure complete collection. The extracted Fe^{n+} ions were then accelerated through a potential difference of 5 kV and then recorded as individual counts by a particle multiplier.

Product Fe^{n+} ions were identified according to charge state n and distinguished from background gas product ions by their different times-of-flight to the multiplier in accordance with their charge to mass ratios. As in our previous work, it was important to ensure that the Fe^{n+} ions were extracted with high and equal efficiency independent of primary beam energy. To achieve this, the pulsed extraction field was subject to a variable delay which could be adjusted according to the transit time of the trailing edge of the electron pulse through the target beam (Shah *et al* 1987).

A time-to-amplitude converter operating with start pulses from the extraction field pulse generator and with stop pulses from the multiplier provided time-of-flight product ion spectra of the type shown in figure 1. Well resolved peaks corresponding to Fe^{n+} formation up to $n = 5$ can be clearly discerned. In this work for electron impact energies up to 1250 eV, an accurate analysis of such spectra was possible for $n = 1$ to 4.

It was important to ensure that the intensity of the Fe atom beam did not change significantly during each series of measurements. A constant intensity could not be

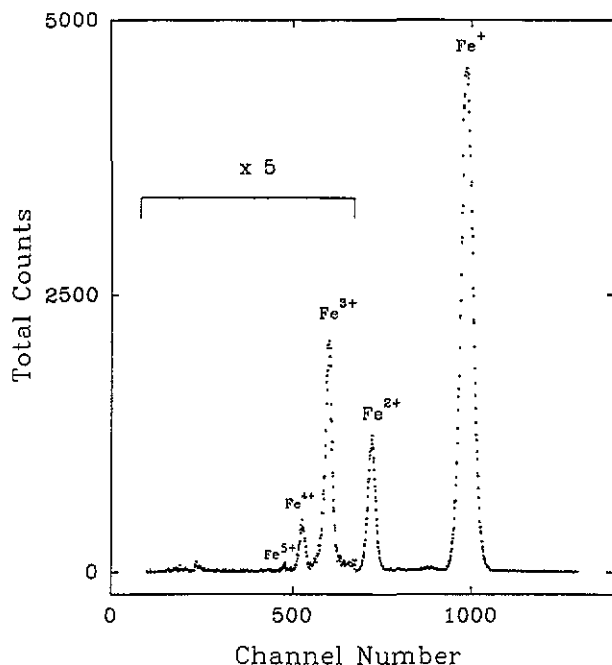


Figure 1. Time-of-flight spectrum showing Fe^{n+} product ions formed in collision of 500 eV electrons with ground state Fe atoms.

ensured simply by controlling the oven temperatures. A reliable indication of the Fe atom intensity was obtained by the use of a pulsed electron beam from a simple electron gun operating at 30 eV. This electron beam was arranged to intercept the Fe atom beam at a point beyond the main crossed beam region and Fe^+ product ions were recorded by a channeltron. This signal was used to monitor any changes in the Fe atom beam flux.

The possibility that the detection efficiency of both the channeltron and the particle multiplier might change due to surface contamination by Fe atoms over the measuring period had to be considered. In order to detect any such changes, a very small amount of helium gas could be fed into the crossed beam chamber so that a He^+ peak then appeared in the time-of-flight spectrum which could be measured relative to the Fe^+ peak. No evidence of change of sensitivity of the detectors was detectable during the measurements.

2.2. Electron beam system

A seven-element electron gun (Shah *et al* 1987) provided pulsed beams equivalent to between 1 and 3 nA in the continuous mode with very small angular divergence. In the interaction region the electron beam had a diameter not exceeding 2 mm while the Fe beam was $6 \times 6 \text{ mm}^2$ square. Careful checks were made to ensure that the effective collision volume was insensitive to the vertical position of the electron beam.

The electron beam current was recorded by a screened Faraday cup located beyond the beam intersection region. The signals from the Faraday cup and from the Fe atom beam monitor were digitized and fed into the microcomputer which also recorded the time-of-flight spectra from the multichannel analyser.

The collision energy of the electron beam can be expressed as $E = V_j - d$ where V_j is the acceleration voltage applied to the midpoint of the V-shaped directly heated filament of the electron gun; d is a correction parameter which allows for filament misalignment and the effect of contact potentials. A value of $d = 1.2 \pm 0.1$ V was obtained by linear extrapolation of the low energy data to the threshold value of 7.9 eV for the ionization of ground state Fe atoms.

2.3. Atom beam source

The oven used to provide the Fe atom beam was similar to that shown in figure 3 of McCallion *et al* (1992b) on our work with Mg. However, in the present work the crucible containing the iron sample (10 mm diameter and 25 mm in depth) was made from type UL1009 high temperature alumina. It was radiatively heated to a temperature of about 1750 °C by means of a surrounding directly heated tungsten tube. The Fe atom beam emerged from the crucible and passed via a defining aperture to the crossed beam region; this was 70 mm from the crucible. At the normal operating temperature of 1750 °C the atom beam density in the crossed beam region was estimated to be $\sim 10^{10}$ atoms/cm³. Under these conditions of operation, the time-of-flight mass spectrum showed no evidence of any contamination of the beam by Fe₂ dimers. With a full charge of iron in the crucible, operation could be sustained for a period of about 10 h.

2.4. Cross section measurements and normalization

For particular electron impact energies within the range 8–1250 eV, the Fe⁺, Fe²⁺, Fe³⁺ and Fe⁴⁺ yields were determined from an average of several measurements of the area of the appropriate peak in the time-of-flight spectrum. Cross sections σ_n for Feⁿ⁺ production are given by

$$\sigma_n = \frac{S_n}{k\mu} \quad (2)$$

where S_n is the Feⁿ⁺ yield per unit electron beam intensity and μ is the effective target thickness of the Fe atoms. The constant k is the overall detection efficiency of the Feⁿ⁺ ions. As in our previous work, a good indication of the independence of k on charge state n was obtained by observing the effect on recorded count rate when the potential difference through which the ions were accelerated to the multiplier tube was increased. The ratios S_4/S_1 , S_3/S_1 and S_2/S_1 were found to become equal and constant when the potential difference through which the ions were accelerated had values in the range 3–5 kV.

While relative cross sections σ_n could be measured with an estimated accuracy within $\pm 5\%$, in order to obtain absolute values using equation (2) it is necessary to determine the product $k\mu$. We have noted previously (McCallion *et al* 1992b) that accurate measurement of μ for thermal energy atom beams of this type is a difficult problem. For this reason, in our previous studies of the ionization of Mg atoms (McCallion *et al* 1992b) we determined the product $k\mu$ by normalizing our relative cross sections σ_1 to the 100–200 eV absolute values measured by Freund *et al* (1990) using the fast crossed beam technique. The absence of metastable atoms in their Mg beams ensured that this was a reliable procedure.

It is inappropriate to use the same normalization procedure in the present work with Fe atoms since (as noted in section 1) Freund *et al* (1990) obtained evidence that

their measured cross sections σ_1 were influenced by the presence of metastable atoms in many possible states. If we do normalize the present relative cross sections σ_1 to those obtained by Freund *et al* (1990) (figure 2) in the range 100–200 eV the two sets of data can be seen to diverge increasingly at energies below about 15 eV. The larger values of Freund *et al* (1990) at these lower impact energies is consistent with a significant metastable atom content. This would also influence the magnitude of the cross section measured at the higher impact energies.

The cross sections σ_2 measured by Freund *et al* (1980) are believed to be much less susceptible to the influence of a metastable atom content. This is because Fe^{2+} production is likely to be dominated (Jacobs *et al* 1980) by Auger processes resulting from the cascade decay of a single vacancy in the *nl* subshells of Fe. For example, Jacobs *et al* (1980) predict that for $3p(M_{II}, M_{III})$ vacancy formation, Fe^{2+} ions are formed with almost unit probability. In this work we have normalized our relative cross sections σ_2 to the corresponding values of Freund *et al* (1990) (figure 3). Both sets of values can be seen to exhibit the same energy dependence over the full energy range of overlap. This excellent agreement provides strong support for our normalization procedure.

Cross sections σ_n normalized in the way described are shown in table 1. The uncertainties associated with individual cross sections are assessed at the 67% confidence level and reflect the degree of reproducibility of the values in terms of the

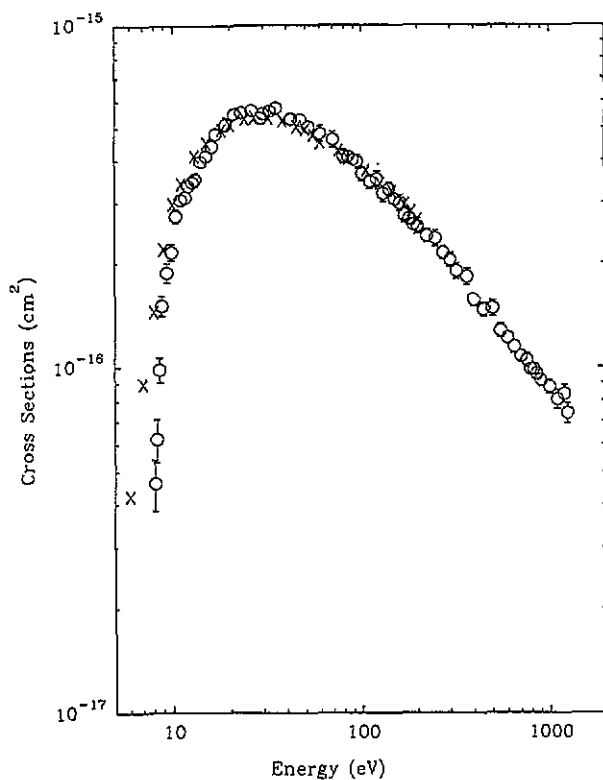


Figure 2. Present relative single ionization cross sections σ_1 (shown O) normalized in the range 100–200 eV to the cross sections σ_1 (shown x) measured by Freund *et al* (1990).

Table 1. Cross sections σ_n for the production of n times ionized iron by electron impact.

Energy (eV)	σ_1 (10^{-16} cm 2)	Energy (eV)	σ_2 (10^{-17} cm 2)	Energy (eV)	σ_3 (10^{-18} cm 2)	Energy (eV)	σ_4 (10^{-19} cm 2)
8.1	0.33 ± 0.05	28.3	0.28 ± 0.06	110	1.48 ± 0.42	250	4.8 ± 1.1
8.3	0.44 ± 0.06	33.3	0.61 ± 0.06	120	1.41 ± 0.21	275	4.7 ± 0.9
8.6	0.70 ± 0.06	35.3	0.74 ± 0.06	130	1.83 ± 0.28	300	7.2 ± 1.2
8.8	1.08 ± 0.07	40.0	0.97 ± 0.12	140	2.53 ± 0.42	325	6.7 ± 1.0
9.4	1.34 ± 0.08	45.0	1.19 ± 0.15	150	2.82 ± 0.42	375	8.2 ± 1.0
9.9	1.54 ± 0.08	50.0	1.39 ± 0.09	170	3.31 ± 0.35	400	7.5 ± 0.9
10.4	1.96 ± 0.09	55.0	1.46 ± 0.12	180	3.73 ± 0.56	450	7.9 ± 1.0
11.0	2.18 ± 0.08	60.0	1.58 ± 0.13	190	3.94 ± 0.35	500	6.7 ± 0.8
11.6	2.22 ± 0.07	65.0	1.86 ± 0.11	200	3.66 ± 0.42	550	6.0 ± 0.8
12.0	2.39 ± 0.10	70.0	1.88 ± 0.11	225	3.66 ± 0.35	650	5.8 ± 0.8
12.6	2.46 ± 0.10	75.0	2.01 ± 0.12	250	4.22 ± 0.28	750	5.2 ± 0.9
13.0	2.50 ± 0.11	80.0	2.18 ± 0.13	275	3.73 ± 0.56	800	5.6 ± 0.9
14.0	2.83 ± 0.11	85.0	2.11 ± 0.13	300	4.29 ± 0.42	850	5.8 ± 0.8
15.0	2.94 ± 0.11	90.0	2.15 ± 0.12	325	4.22 ± 0.42	900	5.3 ± 0.8
16.1	3.15 ± 0.14	100	2.33 ± 0.11	375	4.08 ± 0.28	1000	4.7 ± 0.8
16.8	3.42 ± 0.13	110	2.38 ± 0.11	400	3.87 ± 0.35	1100	4.2 ± 0.8
19.0	3.65 ± 0.17	120	2.35 ± 0.11	450	3.66 ± 0.49	1200	4.4 ± 0.8
21.0	3.91 ± 0.15	130	2.28 ± 0.11	500	3.52 ± 0.28		
23.0	3.95 ± 0.13	140	2.36 ± 0.11	550	3.03 ± 0.21		
26.0	4.01 ± 0.13	150	2.20 ± 0.15	600	2.53 ± 0.28		
29.0	3.80 ± 0.16	170	2.07 ± 0.15	650	2.82 ± 0.21		
30.0	3.92 ± 0.13	180	2.24 ± 0.15	710	2.46 ± 0.21		
32.5	3.98 ± 0.12	190	1.77 ± 0.14	760	2.54 ± 0.21		
35.0	4.08 ± 0.18	200	2.01 ± 0.15	800	2.46 ± 0.21		
42.0	3.77 ± 0.15	225	1.91 ± 0.15	850	2.45 ± 0.14		
47.0	3.76 ± 0.17	250	1.72 ± 0.11	900	2.32 ± 0.14		
52.0	3.58 ± 0.14	275	1.78 ± 0.11	1000	2.15 ± 0.21		
60.0	3.42 ± 0.19	300	1.77 ± 0.09	1100	1.97 ± 0.14		
70.0	3.29 ± 0.18	325	1.78 ± 0.09	1200	1.83 ± 0.14		
80.0	2.93 ± 0.14	375	1.61 ± 0.06				
85	2.93 ± 0.13	400	1.54 ± 0.08				
90	2.87 ± 0.12	450	1.32 ± 0.05				
95	2.83 ± 0.14	500	1.31 ± 0.06				
100	2.60 ± 0.13	550	1.22 ± 0.05				
110	2.46 ± 0.12	600	1.08 ± 0.04				
120	2.51 ± 0.13	650	1.08 ± 0.05				
130	2.27 ± 0.13	710	1.07 ± 0.05				
140	2.34 ± 0.11	760	1.02 ± 0.05				
150	2.19 ± 0.09	800	0.98 ± 0.04				
160	2.14 ± 0.11	850	0.92 ± 0.04				
170	1.97 ± 0.10	900	0.89 ± 0.04				
180	1.92 ± 0.08	1000	0.80 ± 0.05				
190	1.84 ± 0.07	1100	0.77 ± 0.04				
200	1.82 ± 0.09	1200	0.75 ± 0.04				
225	1.70 ± 0.08						
250	1.68 ± 0.09						
275	1.53 ± 0.07						
300	1.46 ± 0.07						
325	1.35 ± 0.07						
370	1.30 ± 0.07						
400	1.12 ± 0.05						
450	1.05 ± 0.05						
500	1.06 ± 0.06						
550	0.91 ± 0.04						

Table 1. (continued)

Energy (eV)	σ_1 (10^{-16} cm 2)	Energy (eV)	σ_2 (10^{-17} cm 2)	Energy (eV)	σ_3 (10^{-18} cm 2)	Energy (eV)	σ_4 (10^{-19} cm 2)
600	0.87 ± 0.03						
650	0.82 ± 0.04						
710	0.77 ± 0.03						
760	0.75 ± 0.04						
800	0.70 ± 0.04						
830	0.70 ± 0.04						
860	0.68 ± 0.04						
900	0.65 ± 0.04						
1000	0.63 ± 0.05						
1100	0.58 ± 0.05						
1200	0.60 ± 0.05						
1250	0.53 ± 0.05						

experimental parameters and statistical fluctuations. The absolute accuracy of our measured cross sections clearly depends on the validity of our normalization procedure and the accuracy of the values of σ_2 measured by Freund *et al* (1990) but cannot be better than $\pm 14\%$.

3. Results and discussion

In figure 3 we show our measured cross sections σ_n for $n = 1$ to 4. Cross sections σ_1 and σ_2 measured by Freund *et al* (1990) for energies up to 200 eV are also included for comparison. While our values of σ_2 are normalized to those of Freund *et al* (1990) their values of σ_1 can be seen to be a factor of about 1.4 larger than our cross sections at 200 eV. At energies near threshold where the influence of metastable atoms should be strong the discrepancy can be seen to be much larger. Included in figure 3 are cross sections σ_1 calculated by McGuire (1977) using the first Born approximation. The calculated values, while larger than our cross sections at energies near the cross section peak, can be seen to agree remarkably well with our values of σ_1 at energies above 700 eV. The fact that similar calculations by McGuire (1977) for both Mg and Ar were also found to be in reasonable accord with our high energy experimental values (McCallion *et al* 1992a, b) also lends further support to the normalization procedure adopted in the present work.

Cross sections σ_n can be seen to attain peak values at progressively higher impact energies with increasing n . At our high energy 1250 eV limit, where each cross section σ_n exhibits roughly the same rate of decrease with increasing energy, equivalent velocity values decrease by less than an order of magnitude as n increases.

We show in figure 3 the threshold energies for removal of one of the 3d, 3p and 3s electrons as calculated by Reilman and Manson (1978) and the L-shell electron removal threshold given by Henke *et al* (1982). At about 13 eV there is evidence of a change of slope in σ_1 corresponding to the energy threshold for removal of a 3d electron. In σ_2 our measured values exhibit a change of slope at about 65 eV corresponding to extra contributions arising from removal of 3p electrons. There is no evidence of significant structure in either σ_1 or σ_2 at energies near the 3s electron removal threshold.

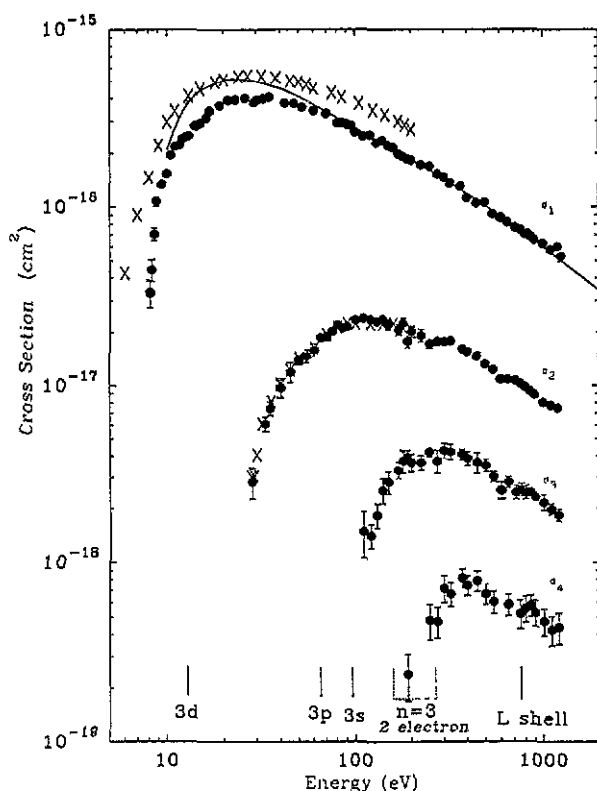


Figure 3. Cross sections σ_n for n times ionization of iron by electrons. ●, $\sigma_1, \sigma_2, \sigma_3, \sigma_4$ present data; ×, σ_1, σ_2 , Freund *et al* (1990); —, σ_1 , theory by McGuire (1977).

At energies of about 700 eV the three cross sections σ_2 , σ_3 and σ_4 exhibit structures that can be attributed to contributions from the ionization of the L-shell electrons. There is evidence of additional structure in σ_2 at about 300 eV which cannot be correlated with any of the single electron removal ionization thresholds. It is possible that this feature may arise as a result of double ionization of $n=3$ electrons. Koike (1992), using the GRASP2 code developed by Parpia *et al* (1992), has recently calculated threshold energies for this process. He has obtained evidence of a number of threshold energies within the narrow energy range 163–270 eV (see figure 3) corresponding to either ionization of two 3s electrons, one 3s plus one 3p electron or two 3p electrons. These calculated thresholds suggest that the well pronounced peak observed around 300 eV in σ_2 does in fact arise from this double ionization process.

4. Conclusion

The present results for Fe show the relative importance of multiple ionization over a wide energy range. Comparison of the present data for the $(1s^2 2s^2 2p^6) 3s^2 3p^6 3d^6 4s^2$ Fe ground state with our previous data for $(1s^2 2s^2 2p^6) 3s^2 3p^6$ Ar and $(1s^2 2s^2 2p^6) 3s^2$ Mg atoms reveals some interesting general features. At 1000 eV total cross sections $\Sigma \sigma_n$ for Fe, Ar and Mg have the not greatly different values of $0.73 \times 10^{-16} \text{ cm}^2$, $0.81 \times 10^{-16} \text{ cm}^2$ and $0.50 \times 10^{-16} \text{ cm}^2$ respectively. The corresponding respective ratios of

σ_3/σ_2 are 0.27, 0.20 and 0.042 and of σ_4/σ_2 are 0.059, 0.045 and 0.002. The not greatly different values of these ratios for Fe and Ar suggests that multiple ionization in these cases is determined mainly by Auger processes with similar branching ratios following the creation of inner shell vacancies within the central core. The much smaller ratios σ_3/σ_2 and σ_4/σ_2 in the case of Mg seem likely to reflect the smaller number of electrons outside the central core available to participate in Auger cascading processes.

Further measurements are planned for other heavy atom targets where current data are sparse or unreliable.

Acknowledgments

This research was supported by a grant from the Science and Engineering Research Council. The Japanese Ministry of Education provided support for one of us (KO) to take part in this work. We are also grateful to Dr F Koike of The School of Medicine, Kitasato University, Japan for making available the results of his recent calculations.

References

- Freund R S, Wetzel R C, Shul R J and Hayes T R 1990 *Phys. Rev. A* **41** 3575
Henke B L, Lee P, Tanaka T J, Shimabukyo R L and Fujikawa B K 1982 *At. Data Nucl. Data Tables* **27** 1
Jacobs V L, Davis J, Rozsnyai B F and Cooper J W 1980 *Phys. Rev. A* **21** 1917
Janev R K 1990 *Report No INDC (NDS)-236/M5* International Atomic Energy Agency, Vienna
Koike F 1992 Private communication
McCallion P, Shah M B and Gilbody H B 1992a *J. Phys. B: At. Mol. Opt. Phys.* **25** 1061
— 1992b *J. Phys. B: At. Mol. Opt. Phys.* **25** 1051
McGuire E J 1977 *Phys. Rev. A* **16** 62
Parpia F A, Grant I P and Fisher C 1992 to be published
Reilman R F and Manson S T 1978 *Phys. Rev. A* **18** 2124
Shah M B, Elliott D S and Gilbody H B 1987 *J. Phys. B: At. Mol. Phys.* **20** 3501
Shah M B, Elliott D S, McCallion P and Gilbody H B 1988 *J. Phys. B: At. Mol. Opt. Phys.* **21** 2751